

Test of the $R(D^{(*)})$ anomaly at the LHC

Syuhei Iguro¹, Yuji Omura² and Michihisa Takeuchi³

¹*Department of Physics, Nagoya University, Nagoya 464-8602, Japan*

²*Kobayashi-Maskawa Institute for the Origin of Particles and the Universe,
Nagoya University, Nagoya 464-8602, Japan*

³*Kavli IPMU (WPI), UTIAS, University of Tokyo, Kashiwa,
Chiba 277-8584, Japan*

Abstract

There are discrepancies between the experimental results and the Standard Model predictions, in the lepton flavor universality of the semileptonic B decays: $B \rightarrow D^{(*)}\ell\nu$. As the new physics interpretations, new charged vector and charged scalar fields, that dominantly couple to the second and third generations, have been widely discussed. In this paper, we study the signals of the new particles at the LHC, and test the interpretations via the direct search for the new resonances. In particular, we see that the $\tau\nu$ resonance search at the LHC has already covered most of the parameter regions favored by the Belle and BaBar experiments. We find that the bound is already stronger than the one from the B_c decay depending on the mass of charged scalar.

1 Introduction

In 2012, the BaBar collaboration has reported that there are large discrepancies in the lepton flavor universalities (LFUs) of the semileptonic B decays: $B \rightarrow D \ell \nu$ and $B \rightarrow D^* \ell \nu$ ($\ell = e, \mu, \tau$). The observables to measure the LFUs are defined as

$$R(D^{(*)}) = \text{Br}(B \rightarrow D^{(*)} \tau \nu) / \text{Br}(B \rightarrow D^{(*)} l \nu) \quad (l = e, \mu), \quad (1)$$

and the experimental results are $R(D) = 0.440 \pm 0.072$ and $R(D^*) = 0.332 \pm 0.030$ [1, 2]. They largely deviate from the Standard Model (SM) predictions: $R(D)_{\text{SM}} = 0.299 \pm 0.003$ and $R(D^*)_{\text{SM}} = 0.258 \pm 0.005$ [3].* The B decays associated with the light leptons are measured with good accuracy, so that the branching ratios of $B \rightarrow D^{(*)} \tau \nu$ are larger than the SM predictions. Interestingly, the Belle collaboration has also reported the excesses in $R(D^{(*)})$ [11–13], although the discrepancies are milder than the BaBar results. Thus, it is expected that those excesses are the new physics signals and there are new particles that couple to the SM fermions flavor-dependently. We note that the LHCb collaboration has also reported only $R(D^*)$ and the latest result is consistent with the SM prediction at the 1σ level [14, 15]. Recently, the Belle experiment also reported the data of the D^* polarization in the $B \rightarrow D^* \tau \nu$ process, and the result is slightly deviated from the SM prediction at 1.5σ level [16].

Motivated by the excesses, several new physics interpretations have been proposed. One simple way to violate the LFU in the B decay is to introduce a field that couples to τ lepton. The field needs to couple to the heavy quarks, bottom and charm quarks, as well. One good candidate for such a field is a charged scalar, H_{\pm} , that has Yukawa couplings with the heavy quarks and heavy leptons [17–32]. The Yukawa couplings are, in general, flavor-dependent, so that we can assume that the couplings with bottom, charm and τ lepton are relatively large, compared to the other elements. Then, the exchange of a charged scalar at the tree-level induces the violation of the LFU. This simple scenario has been proposed just after the announcement of the BaBar result, and the way to prove the new physics directly/indirectly has been widely discussed.

Instead of the charged scalar, we can discuss a charged vector, W'_{\pm} , that dominantly couples to the second and third generations [33–39]. In order to introduce such a vector field, additional gauge symmetry is required and the SM gauge symmetry may be extended. In addition, a non-trivial setup would be necessary to make the W'_{\pm} couplings flavor-dependent. For instance, we can discuss a gauged flavor symmetry or we can expect that some heavy fermions effectively induce the flavorful couplings according to the mass mixing with the SM fermions.

In this paper, we focus on those two new physics interpretations and discuss the consistency with the direct search for the new phenomena at the LHC in the each setup. In particular, it is recently claimed that the charged scalar explanation is in tension with the B_c decay [46–48]. We study the $\tau \nu$ resonance search at the LHC and see that the bound is stronger than the one from the B_c decay.

*See also Refs. [4–10].

We summarize the each explanation in Sec. 2: the H_{\pm} case in Sec. 2.1 and the W'_{\pm} case in Sec. 2.2. Based on the results in Sec. 2, we study the signals at the LHC in Sec. 3. Sec. 3.1 and Sec. 3.2 devote to the analyses of the H_{\pm} and W'_{\pm} scenarios, respectively. We summarize our results in Sec. 4.

2 The explanation of the $R(D^{(*)})$ anomaly

There are large discrepancies between the experimental results and the SM predictions in the LFUs of the semileptonic B decays: $B \rightarrow D^{(*)}\ell\nu$. In the SM, the processes are given by the tree-level diagrams. Then, relatively large new interaction is required to compensate the SM contribution. If there is a heavy charged particle that couples to quarks and leptons flavor-dependently, the following operators could be generated by the heavy particle exchange:

$$\begin{aligned} \mathcal{H}_{eff} = & (C_{SM}^V + C_L^V)(\bar{b}_L\gamma_{\mu}c_L)(\bar{\nu}_{\tau L}\gamma^{\mu}\tau_L) + C_R^V(\bar{b}_R\gamma_{\mu}c_R)(\bar{\nu}_{\tau R}\gamma^{\mu}\tau_R) \\ & + C_L^S(\bar{b}_R c_L)(\bar{\nu}_{\tau L}\tau_R) + C_R^S(\bar{b}_L c_R)(\bar{\nu}_{\tau L}\tau_R) + h.c., \end{aligned} \quad (2)$$

here C_{SM}^V expresses a SM contribution generated by W boson, with $C_{SM}^V = 4G_F V_{cb}^*/\sqrt{2}$. The two terms in the first line can be generated by the W' exchange.[†] The last two terms can be from the H_{\pm} exchange. In this paper, we focus on these two scenarios with the $SU(3)_c$ -singlet mediators. In the following subsections, we review the each new physics scenario and estimate the size of coefficient required by the excesses.

2.1 Charged scalar case

To begin with, we discuss a possibility that charged scalar, H_{\pm} , resides behind the $R(D^{(*)})$ anomalies. The charged scalar can be introduced by adding extra Higgs $SU(2)_L$ doublets. The Yukawa couplings between H_{\pm} and the SM fermions depend on the setup, but in general the scalar couples to all of the SM fermions. Most of the Yukawa couplings are strongly constrained by the flavor physics, so that we have to assume a specific alignment of the couplings. In fact, we limit our Yukawa couplings to those between 2nd and 3rd generations as in [26]. Assuming such a specific parameter choice, we can focus on the $b \rightarrow c$ transition induced by the Yukawa coupling of charged scalar, i.e.,

$$\mathcal{L}_{H_{\pm}} = -H_{\pm} \left\{ Y_R(\bar{b}_R c_L) + Y_L(\bar{b}_L c_R) + Y_{\tau}(\bar{\tau}_R \nu_{\tau L}) \right\} + h.c.. \quad (3)$$

As mentioned above, H_{\pm} is originated from $SU(2)_L$ -doublet scalars, and the neutral components of the doublet also appear as physical fields, after the electroweak symmetry breaking. The masses of the neutral scalars are expected to be around the charged scalar mass (M_H) to evade the constraint from the electroweak precision test [49]. The mixing between a SM Higgs and the additional neutral scalar in this scenario should be tiny [28].

[†]The left-right mixing operator, $(\bar{b}_R\gamma_{\mu}c_R)(\bar{\nu}_{\tau L}\gamma^{\mu}\tau_L)$, would be allowed in general, but we assume that it is not generated by our W' since the W - W' mixing is suppressed.

Then the Yukawa couplings involving the neutral ones are also evaluated as Y_L and Y_R , approximately. When one neutral scalar is denoted as H_0 , the couplings between H_0 and the down-type (up-type) quarks are described as $Y_R V$ ($V Y_L$), where V is the CKM matrix.

Integrating out H_{\pm} , we obtain

$$\mathcal{H}_{H_{\pm}} = -\frac{Y_L Y_{\tau}^*}{M_H^2} (\overline{b_L c_R}) (\overline{\nu_{\tau L} \tau_R}) - \frac{Y_R Y_{\tau}^*}{M_H^2} (\overline{b_R c_L}) (\overline{\nu_{\tau L} \tau_R}), \quad (4)$$

where M_H is the charged scalar mass. Then, we find that Y_R is also strongly constrained by the B_s - \overline{B}_s mixing, taking into account the neutral Higgs exchange at the tree level. As a result Y_R is not useful to improve $R(D^*)$ [26]. We assume $|Y_R| \ll |Y_L|$ in our analysis below. If the charged scalar mass is less than a few TeV, these operators largely contribute to the semileptonic B decay.

The numerical descriptions of $R(D)$ and $R(D^*)$ are given by [19]

$$R(D) \simeq R(D)_{SM} \left\{ 1 + 1.5 \text{Re}[C_L^{\prime S} + C_R^{\prime S}] + |C_L^{\prime S} + C_R^{\prime S}|^2 \right\}, \quad (5)$$

$$R(D^*) \simeq R(D^*)_{SM} \left\{ 1 - 0.12 \text{Re}[C_L^{\prime S} - C_R^{\prime S}] + 0.05 |C_L^{\prime S} - C_R^{\prime S}|^2 \right\}, \quad (6)$$

where $C_I^{\prime S}$ ($I = L, R$) is a normalized coefficient given as $C_I^{\prime S} = C_I^S / C_{SM}^V$, with $C_L^S = -Y_L Y_{\tau}^* / m_H^2$, $C_R^S = -Y_R Y_{\tau}^* / m_H^2$. The required value to achieve the excess of the world average within 1σ is estimated as

$$\frac{|Y_L Y_{\tau}^*|}{M_H^2} \simeq 1.38 \times 10^{-6} [\text{GeV}^{-2}], \quad (7)$$

where, we select the phase of $Y_L Y_{\tau}^*$ to minimize the χ^2 .

The explanation of $R(D^*)$ is, however, constrained indirectly by the B_c decay [46, 47]. The B_c meson decay is easily enhanced by the scalar-type operator. The leptonic decay, $B_c \rightarrow \tau \nu$, is still not observed, but the total decay width and the hadronic decay have been measured and the results are consistent with the SM predictions, although the observables suffer from the large theoretical uncertainty. The authors of Refs. [46, 47] derive the upper bound on the leptonic decay, taking into account the uncertainty, and obtain the upper bound $R(D^*) \lesssim 0.27$ in the charged scalar scenario. The LHCb collaboration has recently reported the consistent $R(D^*)$ results with the SM prediction. The enhancement of $R(D)$ while keeping the $R(D^*)$ consistent to the SM prediction would be only achieved by tuning the phase of $Y_L Y_{\tau}^*$ [26].

2.2 W' case

We can discuss the possibility that the coefficients in Eq. (2) are induced by the heavy vector boson exchange. In the extended SM with extra non-abelian gauge symmetry,

massive extra gauge bosons are predicted. If the SM quarks are charged under the extra gauge symmetry, an extra charged gauge boson, W' , may couple to the third-generation quark and lepton as

$$\mathcal{L}_{W'_I} = W'_{I\mu} \{g_I(\bar{b}_I\gamma^\mu c_I) + g_{I\tau}(\bar{\tau}_I\gamma^\mu \nu_{\tau I})\} + h.c., \quad (8)$$

where, I denotes the chirality: $I = L, R$. The couplings g_I and $g_{I\tau}$ depend on the detail of the setup, and the other couplings involving light SM fermions may arise at the low energy. Assuming the third-generation couplings are dominant, we expect the following operators induced:

$$\mathcal{H}_{W'} = \frac{g_L g_{L\tau}^*}{M_{W'_L}^2} (\bar{b}_L \gamma_\mu c_L) (\bar{\nu}_{\tau L} \gamma^\mu \tau_L) + \frac{g_R g_{R\tau}^*}{M_{W'_R}^2} (\bar{b}_R \gamma_\mu c_R) (\bar{\nu}_{\tau R} \gamma^\mu \tau_R) \quad (9)$$

where $M_{W'_I}$ denotes the W'_I mass. $R(D)$ and $R(D^*)$ are numerically evaluated as [38]

$$R(D^{(*)}) \simeq R(D^{(*)})_{SM} \left\{ |1 + C_L^{\prime V}|^2 + |C_R^{\prime V}|^2 \right\}, \quad (10)$$

where $C_I^{\prime V}$ ($I = L, R$) is a normalized coefficient given as $C_I^{\prime V} = C_I^V / C_{SM}^V$ with $C_L^V = g_L g_{L\tau}^* / m_{W'_L}^2$, $C_R^V = g_R g_{R\tau}^* / m_{W'_R}^2$. In order to accommodate the $R(D^{(*)})$ excesses within 1σ of the world average, the required value of the each coefficient is estimated as

$$\frac{g_L g_{L\tau}^*}{M_{W'_L}^2} \simeq 1.07 \times 10^{-7} [\text{GeV}^{-2}], \quad \frac{g_R g_{R\tau}^*}{M_{W'_R}^2} \simeq 5.55 \times 10^{-7} [\text{GeV}^{-2}]. \quad (11)$$

3 Test of the new physics at the LHC

In this section, we study the signal of the each scenario at the LHC based on the above discussion. In our models, the charged resonances ($V^+ = W'_I^+, H_+$) are produced in association with the third-generation quark and decay to $\tau\nu$ and bc as follows[‡]:

$$g c \rightarrow V^+ b \rightarrow \tau^+ \nu b. \quad (12)$$

The searches for heavy $\tau\nu$ resonances have been performed at the LHC both in ATLAS and CMS experiments [40–43], and severely constrain various models.[§] We numerically found the analysis reported by the CMS collaboration using the data at the LHC Run II with 35.9 fb^{-1} [43] sets the most stringent bound on our models, where they focus on the W' heavier than 400 GeV with the universal couplings to quarks of all generations.

Since the heavy resonances are only couples to the third generation in our models and the spin structures of the H_\pm and the W' are different, the efficiency and the acceptance

[‡]We work in 4 flavor scheme.

[§]Our model focus on the heavy resonance decaying into $\tau\nu$ and it is different from the search for leptoquark using $b + \tau\nu$ in the final state discussed in Ref. [44]. See also Refs. [26, 45].

of the selection cut should be estimated by the simulation. We calculate the acceptances for the case of H_{\pm} and W' using MadGraph5 [50] and PYTHIA8 [51]. The generated events are interfaced to DELPHES3 [52] for the fast detector simulation.

We follow the event selection cuts exploited in [43] as follows:

- exactly one τ -tagged jet, satisfying $p_{T,\tau} \geq 80\text{GeV}$ and $|\eta_{\tau}| \leq 2.4$,
- no isolated electrons nor muons ($p_{T,e}, p_{T,\mu} \geq 20\text{GeV}$, $|\eta_e| \leq 2.5$, $|\eta_{\mu}| \leq 2.4$),
- large missing momentum $\cancel{E}_T \geq 200\text{ GeV}$,
- and it is balanced to the τ -tagged jet: $\Delta\phi(\cancel{E}_T, \tau) \geq 2.4$ and $0.7 \leq p_{T,\tau}/\cancel{E}_T \leq 1.3$, where $\Delta\phi(\cancel{E}_T, \tau)$ is the azimuthal angle between the missing momentum and the τ -jet.

After the above event selection cuts, we plot the m_T distribution and performed the binned log-likelihood analysis using the background m_T distribution [43]. We show the resulting 95 % CL upper bound on the signal cross section times its branching ratio to $\tau\nu$ mode as a function of the resonance mass m_V for each model in Figure 1. The difference of the spin structure provides different upper bounds, for charged scalar (red thick solid), W'_L (blue thick solid), and W'_R (green thick solid). The constraint on the charged scalar case is more stringent than the other cases in most of the m_V region because of the harder m_T distribution.

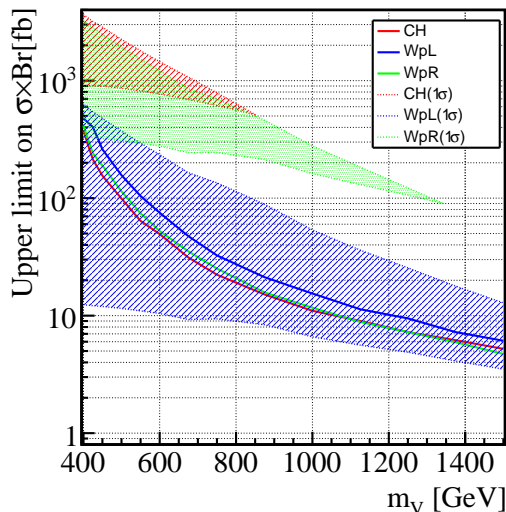


Figure 1: The upper bound on the cross section times branching ratio in the each model at 95% CL. See the main text for the description.

We also overlay the expected signal cross sections in the same plot for the three cases, in the red hatched region (H_{\pm}), in the blue hatched region (W'_L) and in the green hatched

region (W'_R), assuming the couplings are compatible to accommodate the $R(D^{(*)})$ observation in 1σ level. In our models, we can parametrize the cross section with (M, g, g_τ) , where g is the c - b - V coupling and can be taken real without loss of generality; e.g., $(M, g, g_\tau) = (M_H, Y_L, Y_\tau)$, and $(M, g, g_\tau) = (M_{W'_I}, g_I, g_{I\tau})$, respectively. The cross section for the above process is given as follows:

$$\sigma(pp \rightarrow V^\pm) \times Br(V^\pm \rightarrow \tau\nu) = \sigma_0(m_V) \times \frac{|g|^2 |g_\tau|^2}{3|g|^2 + |g_\tau|^2} = \sigma_0(m_V) \times \bar{g}^2 \frac{r}{3 + r^2}. \quad (13)$$

Here, we define the variables, $\bar{g}^2 = |g g_\tau|$, which is related to the $R(D^{(*)})$ prediction, and $r = |g_\tau/g|$. Changing r , while keeping \bar{g} , varies the cross section. We find that basically, the signal cross section is maximized at $r = \sqrt{3}$ when we fix \bar{g} . We also impose the perturbativity of the couplings, i.e. $|g|, |g_\tau| \leq 1$, and r would be constrained as well. We assume $\bar{g}^2 = a_V M_V^2$ to accommodate the $R(D^{(*)})$ observation at 1σ , that is $a_{H^\pm} = 1.36 \times 10^{-6} \text{GeV}^{-2}$, and $a_{W'_L} = 1.07 \times 10^{-7} \text{GeV}^{-2}$. Compared with the required $a_{W'_L}$, a_{H^\pm} needs to be large to accommodate the excess. This stems from small coefficients in Eq. (6). Then we expect the more stringent bound can be obtained for a charged scalar scenario. Since we impose $\bar{g}^2 \leq 1$ due to the perturbativity, M_V exhibits an upper bound 850 GeV for H^+ and 3 TeV for W'_L . The upper boundary of the hatched region is given by $r = \sqrt{3}$ for $\bar{g}^2 \leq 1/\sqrt{3}$ or $r = 1/\bar{g}^2$ ($g_\tau=1$) for $\bar{g}^2 > 1/\sqrt{3}$. The lower boundary of the region is given by $r = \bar{g}^2$ ($|g| = 1$). Note that the lower boundary depends on the upper bound of the allowed couplings.

In the following, we discuss the current status in more detail and the compatibility with the $R(D^{(*)})$ enhancements for each case.

3.1 Charged scalar case

First, we investigate the charged scalar signal at the LHC. As we discuss in Sec. 2.1, the $R(D^{(*)})$ anomaly requires the sizable interaction between the heavy quarks and the τ lepton. In our study of the charged scalar case, there are four free parameters:

$$M_H, Y_L, \text{Re}(Y_\tau), \text{Im}(Y_\tau). \quad (14)$$

The explanation of the $R(D^{(*)})$ anomaly fixes one combination of them, as shown in Eq. (7). Tuning the phase of Y_τ , the bound from the B_c decay can be evaded, although the enhancement of $R(D^*)$ is suppressed. Note that the magnitudes of the Yukawa couplings are not so large and the total decay width is small enough in our study. The production cross section of H_\pm only depends on Y_L , while $|Y_\tau|$ contributes to the branching ratio of H_\pm only. The production cross section times the branching ratio is given by substituting $(M, g, g_\tau) = (M_H, Y_L, Y_\tau)$ in Eq. (13). The exclusion line and the predicted region of the charged scalar case are shown in Fig. 1. As we see the red line and the red hatched region in Fig. 1, the region to accommodate the experimental results on $R(D^{(*)})$ within the 1σ level is already excluded by this $\tau\nu$ resonance search. The light charged scalar region, e.g. $M_H \lesssim 400$ GeV, could achieve the experimental results within the 2σ level.

Fig. 2 shows our predictions on the $R(D)$ and $R(D^*)$ plane for the fixed charged scalar mass, 400 GeV, 500 GeV, 750 GeV and 1000 GeV. The gray region is out of our prediction and the region inside of the black lines is realized by taking Y_L and Y_τ appropriately. Note that the blue, green and red ellipses correspond to the 1σ regions reported by the Belle, BaBar and the HFLAV collaborations. The SM prediction for $R(D)$ and $R(D^*)$ is also marked with the asterisk. In Fig. 2, we also draw the constraints from the B_c decay by the thick magenta lines. Above the magenta line, the leptonic decay of B_c is larger than 30 % and 10 %, so that the region above the line is excluded indirectly. The cyan dashed lines correspond to the predictions by taking $|Y_L| = \pi$.[¶]

The bound from the heavy resonance search at the LHC is our main topic in this paper. We study the excluded parameter region on the $R(D)$ and $R(D^*)$ plane based on Fig. 1. As the signal cross section depends both on Y_L and Y_τ , we have one additional degree of freedom than the product $|Y_L Y_\tau|$. The charged higgs scenario is totally excluded by the $\tau\nu$ resonance search in the light purple region while it would be allowed by tuning the ratio Y_τ/Y_L in the light blue region. Interestingly, we find that most of parameter region is already excluded by the LHC searches. Only for the light charged scalar, $m_H \lesssim 450$ GeV, we can find a parameter region consistent at 1σ by allowing a large $|Y_L| = \pi$. This is because the LHC $\tau\nu$ resonance constraints set more stringent constraints for the heavier resonance. We also stress that the bound by the search at the LHC is stronger than the one by the B_c decay for the considered range $m_H \geq 400$ GeV. In Fig. 3, we also study the excluded parameter region on the Y_L and Y_τ plane based on Fig. 1. The figure on the upper left is for the H_\pm scenario. In the figure, the red line is for the mass of 400GeV. The dotted line express the combination of couplings that accomodate the 1σ of $R(D^{(*)})$. The shaded region is excluded by the collider bound. As is shown in Fig. 2, the H_\pm scenario is constrained stringently. The parameter region for the H_\pm scenario is completely excluded.

3.2 W' case

Next, we study the W' scenario. In the Eq. (8), there are two types of the gauge couplings with the fermions: one is the coupling with right-handed fermions and the other is the one with left-handed fermions. It depends on the charge assignment of the extra non-abelian gauge symmetry. If the extra SU(2) symmetry is assigned to the left-handed fields like the SM SU(2)_L, W'_L only couples to the left-handed fields as well. In a model with W'_R , SU(2)_R symmetry would be assigned to the right-handed fermions. In those cases, W'_I originated from SU(2)_I may mix with W from SU(2)_{L,SM}. The mixing is strongly constrained by the electroweak precision observables, so the mixing should be very tiny. We mainly discuss the case with W'_L in the following for the demonstration. The one with W'_R can be treated in the same way.

In the same way to the charged scalar case, we discuss the $\tau\nu$ resonance originated

[¶]We draw them for an illustration although such a relatively large coupling does not respect the narrow width assumption.

from the on-shell W'_L . Our relevant parameters are

$$M_{W'}, g_L, \text{Re}(g_{L\tau}), \text{Im}(g_{L\tau}). \quad (15)$$

In the same way as the H_{\pm} case, the cross section is given by substituting $(M, g, g_{\tau}) = (M_{W'}, g_L, g_{L\tau})$ in Eq. (13). The exclusion line and the predicted region of the W'_L case are shown in Fig. 1. As we see the blue line and the blue hatched region in Fig. 1, the constraint is not so tight. The exclusion line and the prediction of the W'_R case are also shown as the green line and the green hatched region. As far as the gauge coupling is less than one, the W'_R case is almost excluded unless $m_{W'_R}$ is lighter than 420 GeV, since the gauge coupling required to accommodate $R(D^{(*)})$ anomaly is relatively large compared to the one in the W'_L case. Note that there is no bound from the B_c decay, since the operator is given by the vector-vector coupling in this scenario.

In Fig. 4, our predictions on the $R(D)$ and $R(D^*)$ plane are drawn for fixing W'_I masses at 400 GeV, 500 GeV, 750 GeV and 1000 GeV. The prediction of the W'_I model ($I = L, R$) are along the black line. The 1σ regions reported by the Belle, BaBar and the HFLAV collaborations are depicted by the same color as in Fig. 2. The SM prediction for $R(D)$ and $R(D^*)$ is marked with the asterisk.

We show the possibly surviving region taking the allowed range of the couplings $|g_I| \leq 1$ into account, in the magenta arrows ($I = L$) and in the green arrows ($I = R$). On the magenta thick line, the W'_L scenario is surviving by taking g_L and The parameter region on the magenta dashed line are completely excluded when we require $|g_L| \leq 1$, while it can be survived when we allow $|g_L| \leq \pi$. The green arrows shows the corresponding region for W'_R . In Fig. 3, we also study the excluded parameter region on the $g_{L(R)}$ and $g_{L(R)\tau}$ plane based on Fig. 1. In those figures, the blue(red) lines are for the mass of 1TeV (400GeV). The figure on the upper right (bellow) is for the W'_L (W'_R) scenario. The dotted lines express the combination of couplings that accomodate the 1σ of $R(D^{(*)})$. The shaded regions are excluded by the collider bound. The parameter region for the W'_L is not constrained at all. The parameter region for the W'_R is partially constrained depending on the combination of the couplings.

4 Summary

The discrepancies of $R(D)$ and $R(D^*)$ may be the evidence of new physics behind the SM. The excesses suggest that there are extra fields that couple to quarks and leptons flavor-dependently and the size of the coupling is not so small compared to the W boson coupling in the SM. Motivated by this issue, many new physics interpretations have been proposed, and we find that some of good candidates for the extra fields are charged scalar and charged vector fields. Those extra charged fields are predicted by many new physics models beyond the SM. The charged scalar is, for instance, predicted by many extended SMs with extra $SU(2)_L$ -doublet scalar fields. Extending the SM gauge group is prophetic of some extra massive gauge bosons. The charged vector can be originated from some extra non-abelian gauge symmetry.

Those good candidates have been studied in flavor physics and collider physics. The simple setups, where the heavy charged scalars couple to the light quarks and leptons, have been already excluded, so that some specific structures of the extended SMs are required to achieve the explanations. Such a specific setup makes it difficult to test indirectly and directly by the experiments.

In this paper, we investigate one observable that does not depend on the detail of the setup, that is, the $\tau\nu$ resonance originated from the charged particle. We simply consider each minimal setup in the scalar case and in the vector case, and discuss the consistency between the explanation of $R(D^{(*)})$ and the latest experimental result at the LHC. Interestingly, we found most of the parameter region required by the excesses has been already covered by the resonance search. If the excesses come from the new interactions, the heavy resonances would be relatively light as shown in Fig. 2 and Fig. 4.

Our analysis assumes that the heavy resonances only decay into bc and/or $\tau\nu$. If they decay into the other SM fermions or other particles, the bounds obtained in this paper can be relaxed. Such a case, however, faces stronger bounds from flavor physics, since the couplings with light quarks and leptons are large. Therefore, our results would be applicable as long as the decays to bc and/or $\tau\nu$ are dominant.

It may be interesting to study the bound from the bc resonance search. In the final state, one or two b quarks appear in association with one c quark. Currently, the bound from the di-jet resonance is weaker than that of the $\tau\nu$ resonance search by 1 or 2 order of magnitude [53, 54]. If we can identify the b/c -flavor jet efficiently, we can set stronger exclusion lines [55, 56].

Finally, we comment on the polarization of D^* in the $B \rightarrow D^*\tau\nu$ process. Recently, the Belle collaboration has reported the result on the polarization with high accuracy [16]. This measurement may be useful to test the new physics scenarios motivated by the $R(D^{(*)})$ anomaly. In fact, the possible observables concerned with this problem are recently discussed [57–59]. The more general analysis for the D^* polarization and $R(D^{(*)})$, based on the latest experimental result, will be given near future [60].

Acknowledgments

The work of Y. O. is supported by Grant-in-Aid for Scientific research from the Ministry of Education, Science, Sports, and Culture (MEXT), Japan, No. 17H05404. MT is supported in part by the JSPS Grant-in-Aid for Scientific Research Numbers 16H03991, 16H02176, 17H05399, 18K03611, and the World Premier International Research Center Initiative, MEXT, Japan. The authors thank to Kazuhiro Tobe, Tomomi Kawaguchi, Makoto Tomoto and Yasuyuki Horii for valuable discussions. The authors also thank to David Shih, Matthew Buckley and Poyta Asadi for valuable comments.

References

- [1] J. P. Lees *et al.* [BaBar Collaboration], Phys. Rev. Lett. **109**, 101802 (2012) [arXiv:1205.5442 [hep-ex]].
- [2] J. P. Lees *et al.* [BaBar Collaboration], Phys. Rev. D **88**, no. 7, 072012 (2013) [arXiv:1303.0571 [hep-ex]].
- [3] Y. Amhis *et al.*, [arXiv:1612.07233 [hep-ex]]. See also Heavy Flavor Averaging Group web page for the latest average: “<http://www.slac.stanford.edu/xorg/hfag/>”
- [4] J. F. Kamenik and F. Mescia, Phys. Rev. D **78**, 014003 (2008) [arXiv:0802.3790 [hep-ph]].
- [5] S. Fajfer, J. F. Kamenik and I. Nisandzic, Phys. Rev. D **85**, 094025 (2012) [arXiv:1203.2654 [hep-ph]].
- [6] J. A. Bailey *et al.* [MILC Collaboration], Phys. Rev. D **92**, no. 3, 034506 (2015) [arXiv:1503.07237 [hep-lat]].
- [7] H. Na *et al.* [HPQCD Collaboration], Phys. Rev. D **92**, no. 5, 054510 (2015) [arXiv:1505.03925 [hep-lat]].
- [8] D. Bigi and P. Gambino, Phys. Rev. D **94**, no. 9, 094008 (2016) [arXiv:1606.08030 [hep-ph]].
- [9] D. Bigi, P. Gambino and S. Schacht, JHEP **1711**, 061 (2017) [arXiv:1707.09509 [hep-ph]].
- [10] S. Jaiswal, S. Nandi and S. K. Patra, JHEP **1712**, 060 (2017) [arXiv:1707.09977 [hep-ph]].
- [11] M. Huschle *et al.* [Belle Collaboration], Phys. Rev. D **92**, no. 7, 072014 (2015) [arXiv:1507.03233 [hep-ex]].
- [12] Y. Sato *et al.* [Belle Collaboration], Phys. Rev. D **94**, no. 7, 072007 (2016) [arXiv:1607.07923 [hep-ex]].
- [13] S. Hirose *et al.* [Belle Collaboration], Phys. Rev. Lett. **118**, no. 21, 211801 (2017) [arXiv:1612.00529 [hep-ex]].
- [14] R. Aaij *et al.* [LHCb Collaboration], Phys. Rev. Lett. **115**, no. 11, 111803 (2015) [arXiv:1506.08614 [hep-ex]].
- [15] R. Aaij *et al.* [LHCb Collaboration], Phys. Rev. Lett. **120**, no. 17, 171802 (2018) [arXiv:1708.08856 [hep-ex]].

- [16] Talk by K. Adamczyk on “ B to semitauonic decays at Belle/Belle II” in *CKM 2018*, Heidelberg, Germany, 17-21 September 2018.
- [17] A. Crivellin, C. Greub and A. Kokulu, *Phys. Rev. D* **86**, 054014 (2012) [arXiv:1206.2634 [hep-ph]].
- [18] A. Celis, M. Jung, X. Q. Li and A. Pich, *JHEP* **1301**, 054 (2013) [arXiv:1210.8443 [hep-ph]].
- [19] M. Tanaka and R. Watanabe, *Phys. Rev. D* **87**, no. 3, 034028 (2013) [arXiv:1212.1878 [hep-ph]].
- [20] P. Ko, Y. Omura and C. Yu, *JHEP* **1303**, 151 (2013) [arXiv:1212.4607 [hep-ph]].
- [21] A. Crivellin, A. Kokulu and C. Greub, *Phys. Rev. D* **87**, no. 9, 094031 (2013) [arXiv:1303.5877 [hep-ph]].
- [22] A. Crivellin, J. Heeck and P. Stoffer, *Phys. Rev. Lett.* **116**, no. 8, 081801 (2016) [arXiv:1507.07567 [hep-ph]].
- [23] C. S. Kim, Y. W. Yoon and X. B. Yuan, *JHEP* **1512**, 038 (2015) [arXiv:1509.00491 [hep-ph]].
- [24] J. M. Cline, *Phys. Rev. D* **93**, no. 7, 075017 (2016) [arXiv:1512.02210 [hep-ph]].
- [25] P. Ko, Y. Omura, Y. Shigekami and C. Yu, *Phys. Rev. D* **95**, no. 11, 115040 (2017) [arXiv:1702.08666 [hep-ph]].
- [26] S. Iguro and K. Tobe, *Nucl. Phys. B* **925**, 560 (2017) [arXiv:1708.06176 [hep-ph]].
- [27] K. Fuyuto, H. L. Li and J. H. Yu, *Phys. Rev. D* **97**, no. 11, 115003 (2018) [arXiv:1712.06736 [hep-ph]].
- [28] S. Iguro and Y. Omura, *JHEP* **1805**, 173 (2018) [arXiv:1802.01732 [hep-ph]].
- [29] S. Iguro, Y. Muramatsu, Y. Omura and Y. Shigekami, arXiv:1804.07478 [hep-ph].
- [30] R. Martinez, C. F. Sierra and G. Valencia, arXiv:1805.04098 [hep-ph].
- [31] S. Fraser, C. Marzo, L. Marzola, M. Raidal and C. Spethmann, arXiv:1805.08189 [hep-ph].
- [32] S. P. Li, X. Q. Li, Y. D. Yang and X. Zhang, arXiv:1807.08530 [hep-ph].
- [33] X. G. He and G. Valencia, *Phys. Rev. D* **87**, no. 1, 014014 (2013) [arXiv:1211.0348 [hep-ph]].
- [34] A. Greljo, G. Isidori and D. Marzocca, *JHEP* **1507**, 142 (2015) [arXiv:1506.01705 [hep-ph]].

- [35] S. M. Boucenna, A. Celis, J. Fuentes-Martin, A. Vicente and J. Virto, Phys. Lett. B **760**, 214 (2016) [arXiv:1604.03088 [hep-ph]].
- [36] G. Cvetič, F. Halzen, C. S. Kim and S. Oh, Chin. Phys. C **41**, no. 11, 113102 (2017) [arXiv:1702.04335 [hep-ph]].
- [37] X. G. He and G. Valencia, Phys. Lett. B **779**, 52 (2018) [arXiv:1711.09525 [hep-ph]].
- [38] P. Asadi, M. R. Buckley and D. Shih, arXiv:1804.04135 [hep-ph].
- [39] A. Greljo, D. J. Robinson, B. Shakya and J. Zupan, arXiv:1804.04642 [hep-ph].
- [40] V. Khachatryan *et al.* [CMS Collaboration], Phys. Lett. B **755**, 196 (2016) [arXiv:1508.04308 [hep-ex]].
- [41] CMS Collaboration [CMS Collaboration], CMS-PAS-EXO-16-006.
- [42] M. Aaboud *et al.* [ATLAS Collaboration], Phys. Rev. Lett. **120**, no. 16, 161802 (2018) [arXiv:1801.06992 [hep-ex]].
- [43] A. M. Sirunyan *et al.* [CMS Collaboration], [arXiv:1807.11421 [hep-ex]].
- [44] W. Altmannshofer, P. S. Bhupal Dev and A. Soni, Phys. Rev. D **96**, no. 9, 095010 (2017) [arXiv:1704.06659 [hep-ph]].
- [45] M. Abdullah, J. Calle, B. Dutta, A. Florez and D. Restrepo, arXiv:1805.01869 [hep-ph].
- [46] R. Alonso, B. Grinstein and J. Martin Camalich, Phys. Rev. Lett. **118**, no. 8, 081802 (2017) [arXiv:1611.06676 [hep-ph]].
- [47] A. G. Akeroyd and C. H. Chen, Phys. Rev. D **96**, no. 7, 075011 (2017) [arXiv:1708.04072 [hep-ph]].
- [48] X. Q. Li, Y. D. Yang and X. Zhang, JHEP **1608**, 054 (2016) [arXiv:1605.09308 [hep-ph]].
- [49] T. D. Lee, Phys. Rev. D **8**, 1226 (1973).
- [50] J. Alwall, R. Frederix, S. Frixione, V. Hirschi, F. Maltoni, O. Mattelaer, H.-S. Shao and T. Stelzer *et al.*, JHEP **1407**, 079 (2014) [arXiv:1405.0301 [hep-ph]].
- [51] T. Sjostrand, S. Mrenna and P. Z. Skands, JHEP **0605**, 026 (2006) [hep-ph/0603175].
- [52] J. de Favereau *et al.* [DELPHES 3 Collaboration], JHEP **1402**, 057 (2014) [arXiv:1307.6346 [hep-ex]].
- [53] CMS Collaboration, CMS-PAS-EXO-16-056.

- [54] M. Aaboud *et al.* [ATLAS Collaboration], arXiv:1804.03496 [hep-ex].
- [55] CMS Collaboration, CMS-PAS-BTV-16-001.
- [56] ATLAS Collaboration, ATL-PHYS-PUB-2017-013.
- [57] D. Bardhan, P. Byakti and D. Ghosh, JHEP **1701**, 125 (2017) [arXiv:1610.03038 [hep-ph]].
- [58] A. Azatov, D. Bardhan, D. Ghosh, F. Sgarlata and E. Venturini, arXiv:1805.03209 [hep-ph].
- [59] Z. R. Huang, Y. Li, C. D. Lu, M. A. Paracha and C. Wang, arXiv:1808.03565 [hep-ph].
- [60] S. Iguro, T. Kitahara, R. Watanabe and K. Yamamoto, arXiv:1811.08899 [hep-ph].

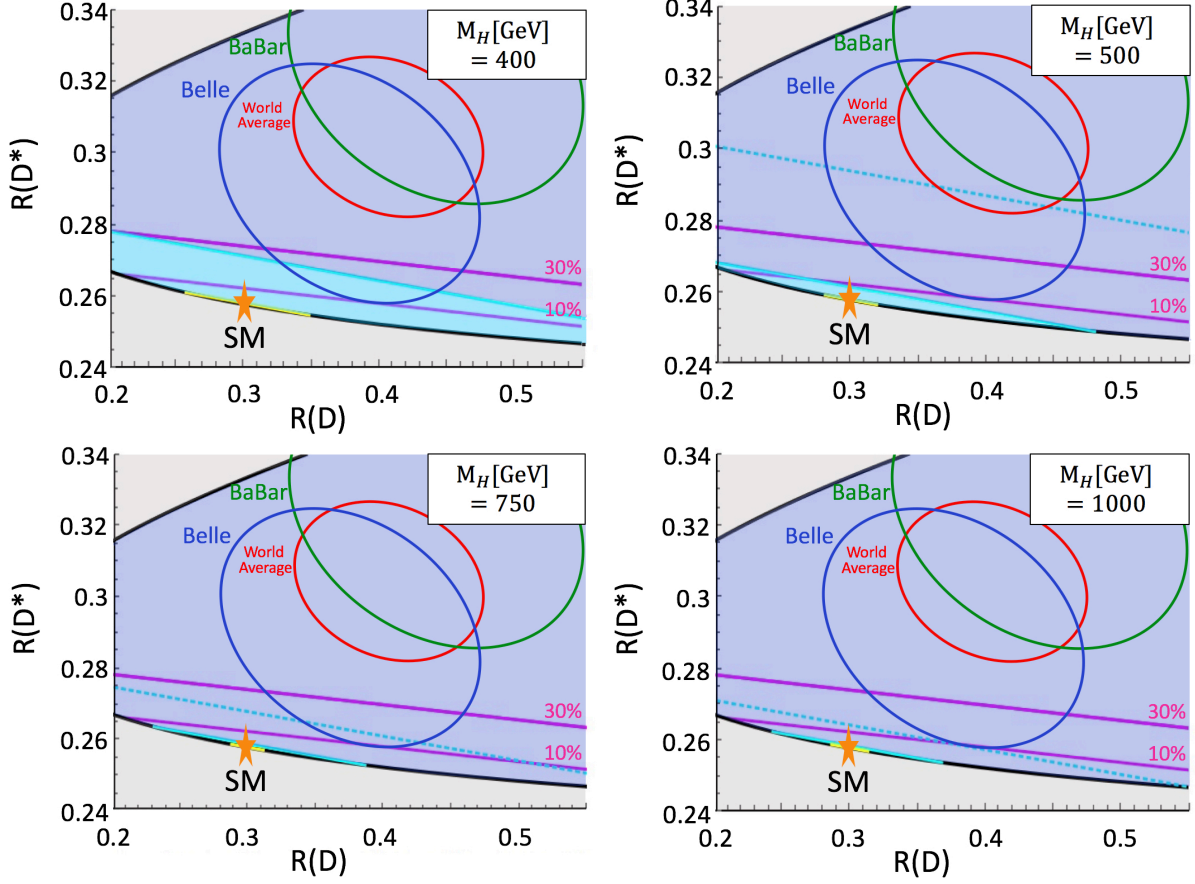


Figure 2: $R(D)$ vs. $R(D^*)$ with the constraints from the B_c decay (magenta lines) and from the charged heavy resonance search at the LHC. The charged scalar masses are fixed at 400 GeV, 500 GeV, 750 GeV and 1000 GeV, as denoted on the each panel. The gray region is out of our prediction and the region inside of the black lines is realized by taking appropriate Y_L and Y_τ . Note that the blue, green and red ellipses correspond to the 1σ regions reported by the Belle, BaBar and the HFLAV collaborations. The SM prediction for $R(D)$ and $R(D^*)$ is marked with the asterisk. The cyan dashed lines correspond to the predictions by taking $|Y_L| = \pi$. In the light purple region, our model is totally excluded by the $\tau\nu$ resonance search. In the light blue region, our model can be allowed by tuning Y_L and Y_τ .

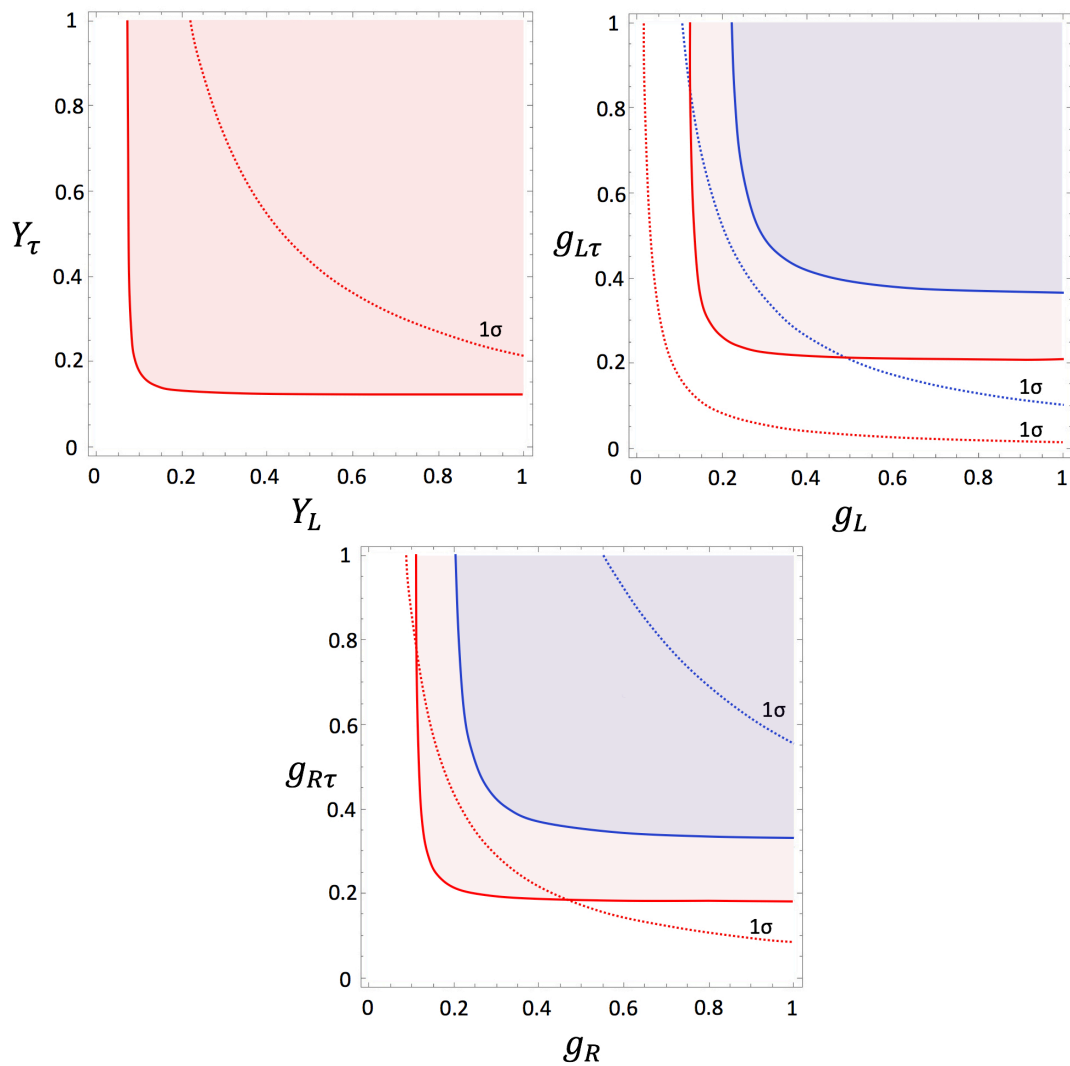


Figure 3: In those figures, the blue (red) lines are for the mass of 1TeV (400GeV). The figure on the left (right) above is for the $H_-(W'_L)$ scenario. The last one on the below is for the W'_R scenario. The dotted lines express the combination of couplings that accommodate the 1σ of $R(D^{(*)})$. The shaded regions are excluded by the collider bound.

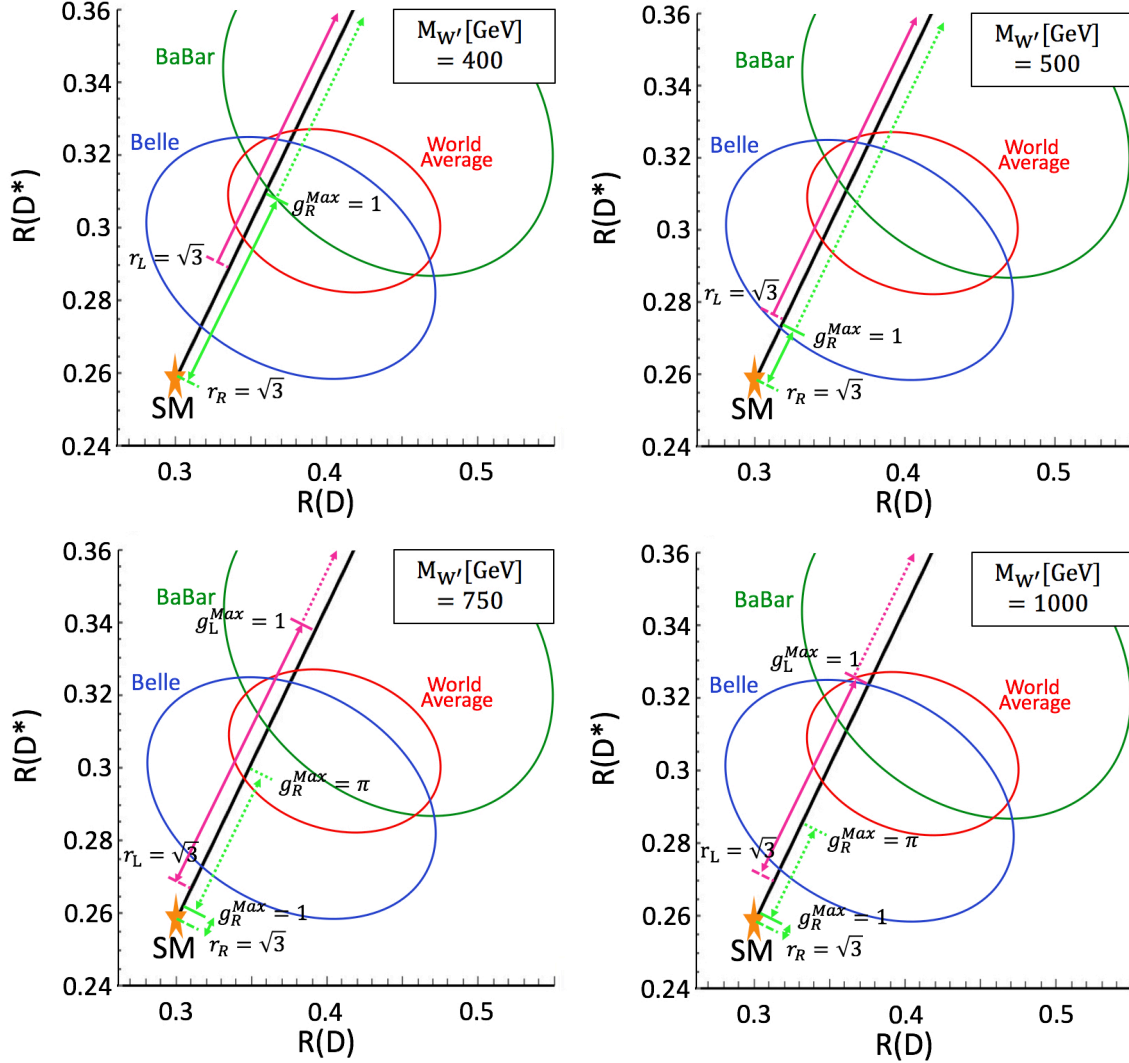


Figure 4: $R(D)$ vs. $R(D^*)$ with the constraint from the charged heavy resonance search at the LHC. $R(D)$ and $R(D^*)$ plane are drawn fixing W'_l masses at 400 GeV, 500 GeV, 750 GeV and 1000 GeV. The prediction of the W'_l model is on the black line. The 1σ regions reported by the Belle, BaBar and the HFLAV collaborations are depicted by the same color as in Fig. 2. The SM prediction for $R(D)$ and $R(D^*)$ is marked with the asterisk. On the magenta thick arrows, the W'_l scenario is excluded depending on g_L and $g_{L\tau}$, assuming $|g_L| \leq 1$. The points on the magenta dashed arrows are excluded as far as $|g_L| \leq 1$ is required but can be survived allowing $|g_L| \leq \pi$. The green arrows show the corresponding cases for the W'_R .